

# INVESTIGATING PRIMARY RUNAWAY ELECTRON GENERATION MECHANISMS WITH TEST PARTICLES IN NON-LINEAR MHD DISRUPTION SIMULATIONS

C. Sommariva<sup>1</sup>, E. Nardon<sup>1</sup>, G.T.A. Huijsmans<sup>1,2</sup>, M. Hoelzl<sup>3</sup>, P. Beyer<sup>4</sup>, D. van Vugt<sup>2</sup>  
and JET Contributors<sup>5,\*</sup>

<sup>1</sup> CEA, IRFM, F-13108, Saint Paul-lez-Durance, France

<sup>2</sup> Dep. Applied Physics, T.U. Eindhoven, P.O.B 513, 5600, Eindhoven, Netherlands

<sup>3</sup> Max-Planck Institute for Plasma Physics, Boltzmannstr. 2, 85768, Garching Germany

<sup>4</sup> Aix-Marseille Université, CNRS, PIIM UMR 7345, 13397, Marseille Cedex 20, France

<sup>5</sup> EUROfusion Consortium, JET, Culham Science Center, Abingdon, OX14 3DB, UK

\* See the author list of 'Overview of the JET results in support to ITER', by X. Litaudon et al., to be published in Nuclear Fusion special issue: overview and summary reports from the 26<sup>th</sup> Fusion Energy Conference (Kyoto, Japan, 17-22 October 2016)

Disruptions are magnetohydrodynamic (MHD) instabilities characterised by a sudden loss of plasma confinement. These instabilities generally lead to high heat loads on the plasma facing components (PFC), stresses on the tokamak structure and the generation of runaway electrons (RE). The latter are electrons having an energy high enough that collisional processes are not able to counteract acceleration by the electric field. In the standard 15MA ITER scenario post-disruptive RE beams are expected to reach currents and energies respectively up to 10MA and 20MJ [1] representing a serious threat to the PFC. Due to the rich MHD activity of a disruption; a full understanding of RE acceleration and deconfinement processes is not achieved yet. Most of the works found in the current literature address as main cause of the generation of the primary runaway seed the acceleration of supra-thermal (Hot Tail [2]) or bulk (Dreicer [3]) electrons caused by the electric field induced by the plasma current decay during the current quench (CQ) phase. Deconfinement by magnetic stochasticity and acceleration by MHD-related electric fields during the thermal quench (TQ) phase are rarely considered although they can strongly influence the RE primary seed production mechanism. In order to investigate these effects, the nonlinear MHD code JOREK [4][5], capable of simulating massive gas injection induced disruptions [6], has been enhanced with a module capable of tracking fast particle full (FO) and guiding center (GC) orbits [7]. First results on electron confinement support the Hot Tail as a mechanism for the generation of the primary RE seed [6] during the TQ, showing that a fraction of the particle initial population is able to survive the TQ phase and to remain confined due to the

reformation of closed magnetic flux surfaces at the CQ onset. Recently, the JOREK fast particle module was improved via the introduction of the collisional drag force derived in [8]. The next section reports details on the drag force model while first results are given in the following section. Conclusions will be stated at the end of this paper.

### Guiding center model extension via collisional drag

The collisional drag model implemented in JOREK is the one presented in [8]:

$$\vec{F}_{coll} = -\frac{q^4}{4\pi\epsilon_0 E_{0,e}} \frac{\gamma((\gamma+1)\alpha_e + \alpha_i)}{(\gamma-1)^{3/2}} \frac{\vec{p}}{m_e c}$$

where  $q$ ,  $\gamma$ ,  $E_{0,e}$ ,  $m_e$ ,  $\vec{p}$  are respectively the particle charge, relativistic factor, rest energy, rest mass and momentum while  $\epsilon_0$ ,  $c$  are the vacuum permittivity and the speed of light.  $\alpha_e$  and  $\alpha_i$  are adapted for the JOREK one fluid model with deuterium (D) massive gas injection taking the forms:  $\alpha_e = n \ln(\Lambda_{ef}) + n_{D_2} \ln(\Lambda_{eb})$  and  $\alpha_i = n \ln(\Lambda_{if}) + n_{D_2} Z_{nucl}^2 \ln(\Lambda_{nucl})$  having defined  $n$ ,  $n_{D_2}$  the plasma and molecular deuterium densities,  $Z_{nucl}$  the deuterium nuclear charge which is set to be two for the extreme case of a collision with the two D nuclei composing a molecule.  $\ln(\Lambda_{ef})$ ,  $\ln(\Lambda_{eb})$ ,  $\ln(\Lambda_{if})$  and  $\ln(\Lambda_{nucl})$  are respectively the Coulomb logarithms for collisional processes with free electrons, impurity bound electrons, plasma ions and impurity nuclei (impurity parameters are taken from the NIST database).

The collisional force is introduced in the GC parallel momentum equation  $\frac{dp_{\parallel}}{dt} = \frac{(p_{\parallel} \nabla \times \hat{b} + q \vec{B})}{\hat{b} \cdot (p_{\parallel} \nabla \times \hat{b} + q \vec{B})} \cdot (q \vec{E} - p_{\parallel} \frac{\partial \hat{b}}{\partial t} - \frac{\mu \nabla B}{\gamma} + \vec{F}_{coll})$  while other equations are left untouched.

### Electron acceleration during the disruption TQ phase

The modified GC model was used for studying the acceleration of fast electrons in the disruption described in [8] and references within. In the present simulations particle populations are initialized as mono-energetic, mono-pitch angle ( $170^\circ$ ) beams having initial

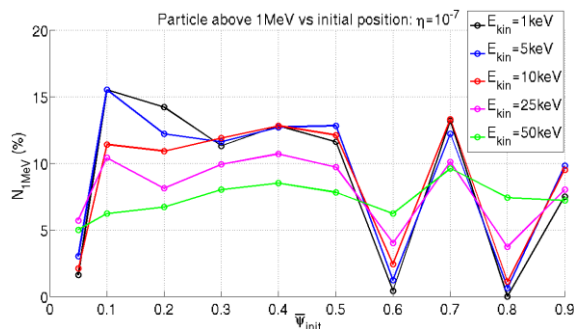


Figure 1: Fraction of particles having final energy above 1MeV as a function of the initial radial position. Different profiles are related to different initial energies.

positions at a given radial distance from the magnetic axis. Simulations start just before the TQ phase and end at the beginning of the CQ (total simulation time  $\sim 2.94$ ms). Figure 1 shows the fraction of particles having a final energy above 1MeV for different initial energies and radial positions. A first analysis of Figure 1 shows that a small fraction of the

initial population not only is able to survive to the disruption TQ but it is also accelerated by

the electric field due to MHD activity. A remarkable feature is that particles are mostly accelerated within the plasma core ( $\bar{\psi} < 0.5$ ) and within the  $m=2$   $n=1$  magnetic island ( $\bar{\psi} = 0.7$ ). A possible explanation to the observed electron acceleration can be found plotting the parallel effective electric field ( $E_{eff,\parallel} = \frac{(p_{\parallel}\nabla\times\hat{b}+q\vec{B})}{|q|\hat{b}\cdot(p_{\parallel}\nabla\times\hat{b}+q\vec{B})} \cdot (q\vec{E} + \vec{F}_{coll})$ ) for a pitch angle of  $170^\circ$  and energies of 1 and 10 keV at the TQ and CQ onset (Figures 2 and 3). Figure 2 shows that during the TQ the effective electric field presents a cellular topology with an alternation of accelerating (blue) and decelerating (red) cells. This topology gradually disappears when the disruption enters the CQ phase (Figure 3). Moreover, Figure 3 clearly shows that particles having energies of 1keV are not accelerated by the electric field caused by the plasma current decay (dominant collisional drag). The presence of electric field during the TQ, the impossibility of accelerating electrons having energy of 1keV during the CQ and the generation of REs at the end of this simulation suggest that fractions of the initial electron population might experience

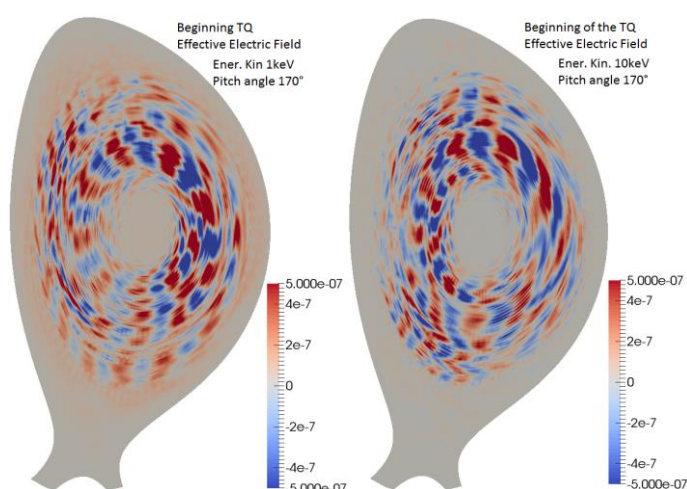


Figure 2: Effective electric field (in dimensionless units) at the beginning of the TQ for a pitch angle of  $170^\circ$  and energies of 1keV (left) and 10keV (right). Blue and red are respectively regions of accelerating and decelerating effective electric field.

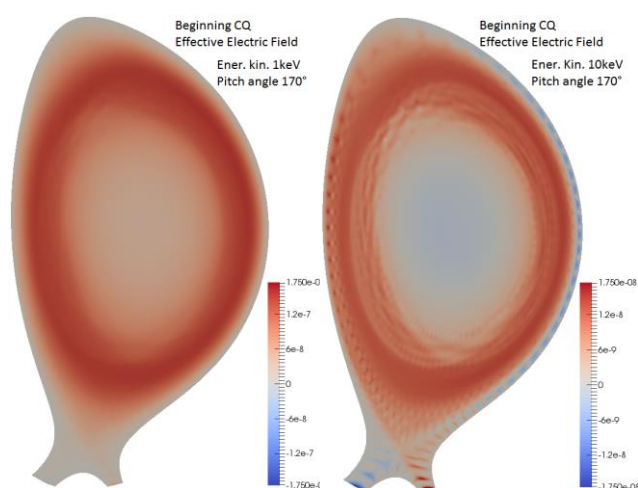


Figure 3: Effective electric field (in dimensionless units) at the beginning of the CQ for a pitch angle of  $170^\circ$  and energies of 1keV (left) and 10keV (right). Blue and red are respectively regions of accelerating and decelerating electric field.

acceleration or deceleration when being respectively influenced by accelerating or decelerating electric field cells. When magnetic perturbations start to decay, electrons accelerated by electric cells might remain confined due to the generation of closed magnetic flux surfaces and be brought to runaway conditions during the CQ phase. This view seems to be in agreement with the GC energy profiles reported in Figure 4 (initial radial position  $\bar{\psi} = 0.7$  and

kinetic energy 1keV) which shows that most of the initial electrons (blue lines) experience a decrease of their energy due to collisional drag while a fraction of them are deconfined (green lines) or become REs (red lines). Finally, previous investigations without collisional drag [7] suggest that electron deconfinement is more effective as the electron energy increases, which might be in agreement with the fact that the fraction of the electron population having a final energy above 1MeV varies with the increase of the initial population energy (Figure 1). This might be related to the existence of an optimal region in phase space where the likelihood of an electron to be confined and become REs is maximized.

### Conclusions

The GC model of the JOREK fast particle tracker has been extended via the introduction of a collisional drag force. First applications on disruption simulations show that electrons might be accelerated during the thermal quench phase of a disruption. This is related to the presence of accelerating electric field cells at the point of maximum MHD activity which can bring electrons to energies high enough for becoming REs during the CQ phase. The proposed mechanism, usually not taken into account in the current literature [9], might reinforce the RE primary seed obtained via the Hot Tail mechanism. It should be noted that during the JET disruption simulated here no RE plateau was seen. Further quantitative validation of the MHD simulations will be required to ensure electron deconfinement and electric field are not under- or overestimated. This will be addressed via direct comparisons to experiments.

### Acknowledgments

This work has been carried out within the framework of the EUROfusion Consortium and has received funding from the Euratom research and training programme 2014-2018 under the grant No 633053. The views and opinions expressed herein do not necessarily reflect those of the European Commission.

### References

- [1] M. Lehnen et al., *J. Nucl. Mater.*, vol. 463, p. 39, 2015
- [2] H. Smith et al., *Phys. Plasmas*, vol. 12, p. 122505, 2005
- [3] J. W. Connor and R. J. Hastie, *Nucl. Fusion*, vol. 15 p. 415, 1975
- [4] G. T. A. Huysmans and O. Czarny, *Nucl. Fusion*, vol. 47, p. 659, 2007
- [5] O. Czarny and G. T. A. Huysmans, *J. Comp. Phys.*, vol. 227, p. 7423, 2008
- [6] E. Nardon et al., *Plasma Phys. Control. Fusion*, vol. 59, P. 014006, 2017
- [7] C. Sommariva et al., arXiv:1704.08955 (submitted to Nucl. Fusion), 2017
- [8] J. R. Martin-Solis et al., *Phys. Plasma*, vol. 22, p. 092512, 2015
- [9] J. R. Martin-Solis et al., *Nucl. Fusion*, vol. 57, p. 066025, 2017

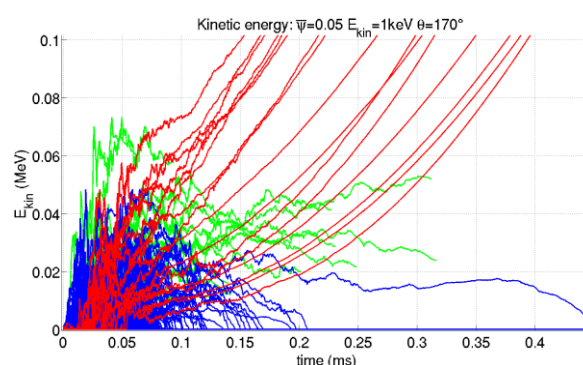


Figure 4: GC energy time profiles during the TQ: blue, red and green lines are respectively GC having final energy below 1MeV, above 1MeV and deconfined during the TQ.